Simulation of Smith-Purcell radiation using a particle-in-cell code

J.T. Donohue, J. Gardelle

▶ To cite this version:

Simulation of Smith-Purcell radiation using a particle-in-cell code

J. T. Donohue

Centre d'Etudes Nucléaires de Bordeaux-Gradignan, BP 120, 33175 Gradignan, France

J. Gardelle

CEA CESTA, BP 2, F-33114 Le Barp, France
(Received 12 April 2005; published 24 June 2005)

A simulation of the generation of Smith-Purcell (SP) radiation at microwave frequencies is performed using the two-dimensional particle-in-cell code MAGIC. The simulation supposes that a continuous, thin (but infinitely wide), monoenergetic electron beam passes over a diffraction grating, while a strong axial magnetic field constrains the electrons to essentially one-dimensional motion. The code computes the time-dependent electric and magnetic fields by solving the Maxwell equations using a finite element approach. We find that the passage of the beam excites an evanescent electromagnetic wave in the proximity of the grating, which in turn leads to bunching of the initially continuous electron beam. The frequency and wave number of the bunching are determined, and found to be close to those proposed by Brau and co-workers in recent work. This frequency is below the threshold for SP radiation. However, the bunching is sufficiently strong that higher harmonics are clearly visible in the beam current. These harmonic frequencies correspond to allowed SP radiation, and we see strong emission of such radiation at the appropriate angles in our simulation, again in agreement with Brau's predictions. We also find that at the ends of the grating, some of the evanescent wave is diffracted away from the surface, and radiation below the threshold occurs. In addition, we observe a second evanescent wave at the same frequency, but with a different wave number. The existence of this wave is also predicted by the theory, although its presence in our simulation is unexpected. Numerical estimates of the growth of the evanescent wave are also in reasonable agreement with the predictions, although the precise form of the dependence of the gain on beam current remains hard to establish.

I. INTRODUCTION

In 1953 Smith and Purcell [1] sent an electron beam of energy about 300 keV along the surface of a diffraction grating, and observed visible radiation, which satisfied the condition they proposed,

$$\lambda = \frac{L}{n}\left(\frac{1}{\beta} - \cos\theta\right), \qquad (1)$$

where λ denotes the wavelength of the radiation produced at angle θ with respect to the beam, L is the grating period, and n is an integer. We write $\beta = v/c$, where v denotes the electron's velocity, and c the speed of light. Smith and Purcell (SP) verified that the radiation indeed satisfied their condition, they observed several harmonics, and made an estimate of the intensity of the radiation based on a simple picture of a radiating dipole, all with notable brevity. Subsequent work by van den Berg [2] provided a more detailed description of the phenomenon. Shortly thereafter appeared several articles in whose titles Smith-Purcell was accompanied by the phrase free electron laser (FEL). These works [3,4] suggested that the SP effect, if it could be made coherent through beam bunching, would provide an intense but compact source of tunable radiation. Subsequently Walsh and co-workers developed a SP FEL that produced radiation in the Terahertz (THz) range [5]. At present several other projects that use low energy (30–

100 keV) beams are either functioning [6] or in preparation [7]. At higher beam energies (a few MeV) results have been obtained by several groups, for example, in Mainz [8] and Frascati [9].

On the theoretical side, two recent contributions have been proposed which find results differing from those of Schächter and Ron in Ref. [4]. Kim and Song [10] consider a sheet beam passing close to a grating. They suggest that both an evanescent and a propagating mode may have the same frequency. The electron beam excites the evanescent mode, which, under the influence of the grating, scatters into the propagating mode, the latter then escaping as SP radiation. They find the gain to be proportional to $\sqrt{I}$, where I denotes the beam current, whereas Schächter and Ron predicted gain $\propto I^{1/3}$. A different treatment was proposed by Andrews and Brau [11], and enlarged upon in subsequent work [12]. Here the analysis assumes a rectangular grating of arbitrary form, while the space above the grating is filled by uniform plasma. First the authors establish the dispersion relation for the electromagnetic field in the two regions, using Floquet theory. While the problem involves finding the roots of an infinite determinant, Andrews and Brau show that under normal conditions it is sufficient to find the roots of a function of two variables, the frequency ω and the wave number k. With the aid of a symbolic manipulation program such as MAPLE or

MATHEMATICA, one may easily verify their results. It turns out that the dispersion relation allows only evanescent solutions. Next the operating point is fixed by the intersection of the dispersion curve with the beam line, $\omega = c\beta k$. The coupling of the beam and structure then follows the path established long ago by Pierce for traveling-wave tubes [13]. Andrews and Brau find the corresponding result, with a gain which follows the $I^{1/3}$ law. However, their coefficient differs from that of Schächter and Ron. But the most important point is that the frequency they find is never great enough to satisfy the SP condition. While all previous analyses assumed that the evanescent wave oscillates at an allowed SP frequency, Andrews and Brau argue that this cannot happen. The scenario they propose is the following. The beam excites the evanescent wave, which exists only in the neighborhood of the grating. The axial component of the electric field causes bunching of the beam with the same frequency, axial wavelength, and gain. The bunching grows strong enough for harmonics of the fundamental frequency to appear. Standard SP radiation is emitted by the individual electrons. At angles such that the SP frequency is equal to an integer multiple of the beam bunching frequency, coherent (proportional to N_e^2, where N_e denotes the number of electrons) SP radiation may occur, with far greater intensity than incoherent radiation. An important point, clearly exposed in Ref. [12], is that coherent SP emission is a collective effect requiring several bunches to emit coherently.

In their analysis of the Dartmouth experiments of Walsh and collaborators [14], Brau and his colleagues find in addition that the intersection of the beam line with the dispersion curve occurs at a point where the group velocity $d\omega/dk$ is negative. This means that the system functions in a manner similar to a backward wave oscillator, where the energy in the wave moves upstream toward the incoming electron beam. While this is not a general rule, it is typical of very low energy devices, since the beam line has a small slope and will intersect the periodic (in k) dispersion curve in its descending portion. Backward wave devices have intrinsic positive feedback, since the incoming unbunched electron beam encounters a wave that has grown strong in traversing the grating.

Given the different viewpoints on the production of coherent SP radiation, we decided to investigate the problem using a standard tool, the particle-in-cell (PIC) code MAGIC. Having access to the two-dimensional version, which is consistent with the analytic treatments cited above, and being used to simulating microwave devices with it, we felt that it could be relied on to provide support for one or the other of these differing views. Accordingly, we chose to work in the microwave domain, using a simple rectangular grating of period 2 cm, with grooves 1 cm deep and 1 cm wide. A strong axial magnetic field is used to impose nearly axial motion on the electrons, which are emitted in a narrow monoenergetic (100 keV) beam 2 mm above the grating.

We note that some earlier work on simulating the SP effect with a PIC code was performed by Hirata and Shiozawa [15]. The questions we are concerned with were not investigated in that work. We mention also the recent analytic work of Freund and Abu-Elfadi on the Smith-Purcell traveling-wave tube [16], which resembles that of Andrews and Brau, except that there is a second conducting plane parallel to the grating. While the analysis of the coupling of beam and structure modes is similar, the presence of the second conductor means that radiation occurs only in the forward and backward directions, and the possibility of coherent SP radiation at a particular angle is lost.

This paper is organized as follows: In Sec. II a brief description of the MAGIC code is presented. The details and principal results of our simulation are given in Sec. III. Finally, in Sec. IV, we attempt to interpret and compare our results using the theories outlined above. We find that the picture proposed by Brau and his collaborators is close to what our simulation finds, although we note that the presence of a large-amplitude evanescent wave at the same sub-SP frequency but different wave number complicates the interpretation of our results.

II. DESCRIPTION OF THE NUMERICAL ANALYSIS

Precise understanding of an experiment involving an intense electron beam interacting with electromagnetic fields requires, in general, recourse to numerical simulations. For example, in high-power microwave tubes (HPM), the effects of beam space charge, which dominate the physics, cannot be treated with simple linear theories. The beam behavior, as well as the saturation mechanisms of the emitted radiation, is best investigated using numerical tools such as particle-in-cell (PIC) codes. While some laboratories have developed their own codes, several commercial software packages are also available. At CEA/CESTA, the code MAGIC [17] has been used to simulate HPM sources in the GHz range of frequencies. Although the frequencies of the recently performed SP experiments fall generally in the THz range, we choose to simulate the coherent SP radiation in the few GHz regime, since that is where we have prior experience with the code. Since the essential physics is independent of the frequency, we expect our results to have general validity.

From the reference manual, we extract the following description of the code: MAGIC is a 2D/3D electromagnetic PIC code, i.e., a finite-difference, time-domain code for simulating plasma physics processes. These processes involve interactions between space charge and currents and electromagnetic fields. Beginning from a specified initial state, the code simulates a physical process as it evolves in time. The full set of Maxwell's time-dependent equations is solved to obtain electromagnetic fields. Similarly, the complete Lorentz force equation is solved to obtain rela-

tivistic particle trajectories, and the continuity equation is solved to provide current and charge densities for Maxwell's equations. This approach provides self-consistency and is applicable to broad classes of plasma physics problems. Our version of the code is two-dimensional; it assumes that all fields and currents are independent of the z coordinate. However, the motion of electrons is calculated in three dimensions.

A. Geometry and parameters of the SP simulation

In Fig. 1, we display the geometry we have chosen for our 2D Cartesian simulation, where the electron beam propagates in the x direction. The setup includes a perfectly conducting grating in the center at the bottom, a small cathode which emits beam, and a vacuum box in which radiation propagates. The boundary includes hatched regions. In these areas, which the MAGIC language calls "free-space regions," the electromagnetic fields are absorbed without reflection, provided they are thick enough. We also tried conducting enclosure walls in our early attempts, but excessive reflection at the metallic surfaces made it difficult to interpret our results.

In this 2D calculation the z axis is ignored, so that quantities like charge density or current are understood as per meter in the z direction. The box is divided into a mesh consisting of rectangular cells. They are chosen very small in the region where the beam propagates, medium in the grating and large in the remainder of the box. Our grating has a simple rectangular form as in the model of Andrews and Brau. We use a thin solid beam, and place its edge 2 mm above the top of the grating. While we could safely reduce this distance in our simulation, it seems unrealistic to try to get much closer to the grating with an intense beam without provoking damage. In their analysis, Andrews and Brau supposed that the entire region above the grating was filled with uniform beam, while Kim and Song assumed a beam of infinitesimal thickness. Our simulation is somewhat intermediate between these two extremes. The main parameters of the simulation are summarized in Table I.
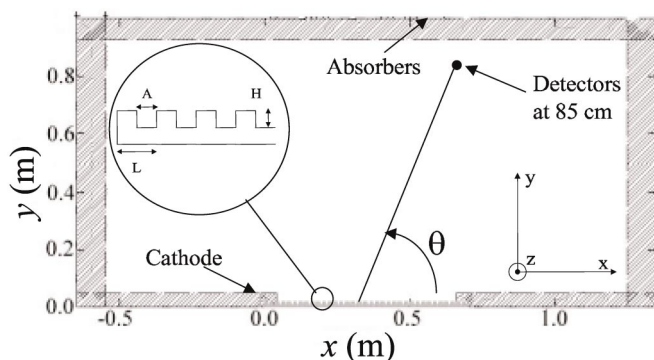
TABLE I.   The main parameters of our SP simulation.

Electron beam energy (injection)	$E = 100$ keV
Current	$25 < I < 1500$ A
Beam thickness	$\delta = 5$ mm
Beam-grating distance	$e = 2$ mm
Grating period	$L = 2$ cm
Maximum wave number	$K = 2\pi/L = \pi$ cm^{-1}
Grating groove depth	$H = 1$ cm
Grating groove width	$A = 1$ cm
Number of periods	$N = 35$
External magnetic field	$B_x = 2$ T

The MAGIC algorithm, which produces electron emission from the cathode, is chosen to obtain a perfect laminar beam, with a smooth rise time of 2 ns. A superimposed constant magnetic field of 2 T (in the x direction) ensures stable beam propagation above the grating. In the rest of this paper, only the beam current will be varied.

B. Numerical diagnostics

MAGIC possesses a large set of commands that allow us to access the relevant physical quantities such as electron phase-space trajectories, electromagnetic fields as functions of space or time variables and related macroscopic quantities, such as field energy in the box, or power outflow. In the framework of our SP simulation, the main output data we use are the following:

(i) Plots of the beam current vs time at different x values, which give information on beam bunching (OBSERVE command in MAGIC). Similarly, plots of the current as a function of x at fixed time permits us to estimate the spatial parameters of bunching (range field command in MAGIC).

(ii) Simulated detectors record the time history of the magnetic field component B_z close to the boundaries of the simulation box. They allow us to study SP radiation, both in amplitude and frequency, as a function of the observation angle. This latter is varied by steps of 1° (the origin is chosen at the center of the grating) and the distance to each observation point is 85 cm, as indicated in Fig. 1.

(iii) Two-dimensional contour maps of B_z, throughout the box at a given time, permit us to observe the radiation pattern. Comparison of such maps at nearby times reveals interesting features, providing information as to the source of the radiation fields.

III. RESULTS OF THE SIMULATION

A. Sub–Smith-Purcell radiation

In the basic SP equation [Eq. (1)], the maximum wavelength that can occur, for a given β, is $\lambda_{max} = L(1/\beta + 1)$. For our nominal energy of 100 keV, $\beta = 0.548$, and with $L = 2$ cm, the maximum wavelength is 5.65 cm. In our first simulations, we found copious radiation at a wavelength of 6.5 cm (4.6 GHz), which exceeds the maximum

FIG. 1.   Geometry used in MAGIC to calculate SP radiation.

SP value. In addition, this radiation was not very directional, emerging to some extent at all angles. In order to see genuine SP radiation, we had to introduce the free-space boundary conditions of MAGIC, and eliminate as much as possible metallic surfaces (except the grating). This reduced the amount of the 6.5 cm radiation (which we shall henceforth refer to as sub-SP) sufficiently for us to see radiation at approximately 3.25 cm, of frequency 9.2 GHz. This radiation was strongest at the associated angle of 78°, where the SP relation predicts it.

In order to understand the origin of this sub-SP radiation we have followed the analysis of Andrews and Brau (we calculate using a 4×4 approximation to their infinite determinant) to find the dispersion relation for our grating. The result is shown in Fig. 2, in the limit of zero plasma frequency. The abscissa is $k/2\pi$ and the ordinate is $f = \omega/2\pi$, where k is the axial wave number and ω the angular frequency. We show also the beam line, $\omega = c\beta k$, whose intersection with the dispersion curve (labeled P in Fig. 2) yields the wave number and frequency of the evanescent wave. The intersection occurs for $k/2\pi = 28.17$ m^{-1}, $f = 4.63$ GHz. This frequency is close to that of the sub-SP radiation we find in the simulation. The wave is evanescent, behaving like $e^{-\alpha y}$, where this calculation predicts $\alpha = 1.48$ cm^{-1}. We note that at the intersection $d\omega/dk < 0$, i.e., the group velocity is negative. It is clear that for a given frequency, there exists a second evanescent mode (labeled P' in Fig. 2), whose wave number in our case is 1.37 cm^{-1}. (One can show, using the Andrews and Brau expression that if k satisfies the dispersion relation for a given ω, $k' = K - k$ does also). Since the dispersion relation is invariant under $k \rightarrow -k$ there are a total of four modes possible for a given allowed frequency, i.e., $k, k', -k, -k'$. As we shall see, these three other modes are present in the simulation, even though they are not resonant with the beam. Also shown on the figure is a set of points found empirically using MAGIC. A line current source operating at fixed frequency was inserted in a groove near the upstream end of the grating, and was activated for several ns, until the evanescent wave reaches the other end. Using finite Fourier transforms (FFT) the spatial wave number of this propagation was determined, and at each frequency, two such wave numbers were observed. These points are seen to fit the theoretical curve rather well; typical discrepancies are <1% .

We consider the sub-SP radiation we see to be a direct consequence of this evanescent wave. When the wave reaches the end of the grating, both a reflected (with wave number $-k$) and a scattered wave at the same frequency will be generated. The second evanescent wave (at wave number $-k'$) is also apparently generated by reflection. The diffraction from the grating ends is the sub-SP we observe. This radiation was apparently not observed in the Dartmouth SP FEL experiment. We conjecture that our 2D simulation may not be a reliable guide to the scattered sub-SP radiation in a 3D experiment. In order for a 2D treatment to be valid, it would probably be necessary to have the beam extend at least a few wavelengths along the z direction. In addition, the second evanescent wave, which falls off more slowly in y than the usual one, may be the source of the copious sub-SP radiation we see emitted at the upstream end of the grating.

The mechanism that leads to coherent−Smith-Purcell (CSP) radiation is beam bunching, just as in all coherent radiation sources that use intense electron beams. CSP radiation arises when a harmonic of the sub-SP wave matches a permitted SP wavelength. It will give rise to a strong emission at selected angles.

B. Results at 100 A

Here we analyze the simulation with a beam current of 100 A. Notice that this is the current per meter in the z direction. It corresponds to a realizable current density of 2 amp/cm^2. Evidence of CSP emission is displayed in Fig. 3, which shows the 2D contour map of B_z at 34 ns (close to the time at which saturation occurs). For reasons of dynamic range, this map is composed out of five individual slices. Most of the radiation at 9.1 GHz is found in a band near the expected angle of 78°. (As will be shown later, the mean beam velocity at this time is somewhat less than the theoretical value, and the corresponding emission angle is reduced to about 74°.) One sees clearly that its period is approximately the theoretical value of 3.25 cm; it corresponds to the second harmonic of the evanescent mode. In addition to this SP radiation there is a large background of the sub-SP radiation at 6.5 cm over a large
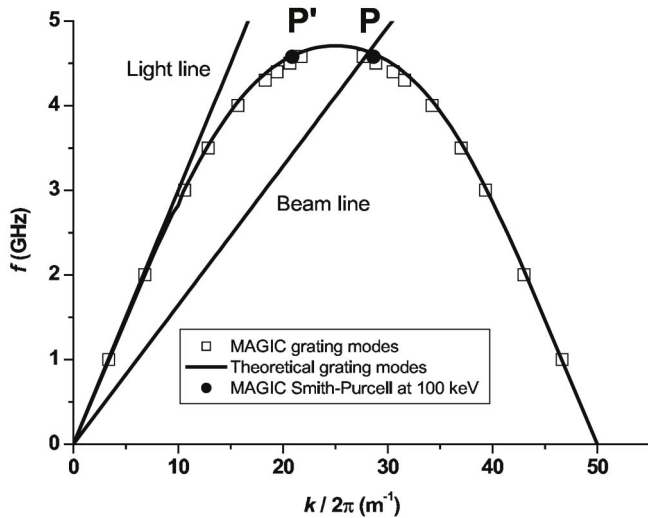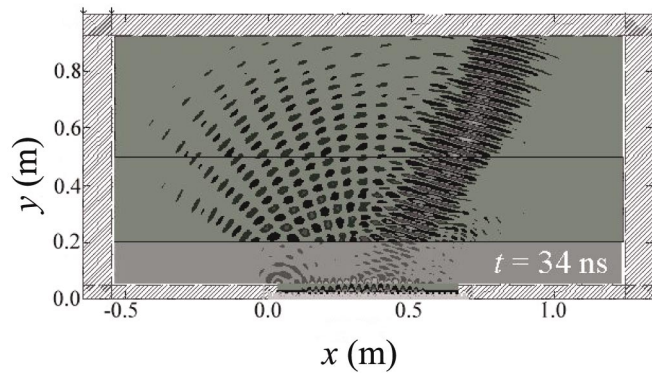

FIG. 2. Dispersion relation for our grating and intersection with the beam line. The operating point P is shown, as well as a second point P' which has the same frequency but $k' = K\text{-}k$. The open squares indicate the results of a MAGIC simulation in which a fixed frequency current source is placed in a groove and excites the evanescent waves. The two wave numbers corresponding to each frequency are found by FFT.

FIG. 3.   *x-y* contour map of B_z obtained at 34 ns.

range of emission angles. The radiation pattern at this instant is quite similar to that of a two-slit interference experiment. Indeed, the separation between angles of zero intensity is rather close to the simple estimate of 5.4° given by path-length differences for two coherent sources emitting at 4.6 GHz separated by 70 cm. However, not all maps show such a clear interference pattern.

The B_z detector placed at 85 cm and 64° from the grating center is inside the CSP emission slice. Its temporal behavior is given in Fig. 4, along with the corresponding FFT. We point out that the code calculates the total magnetic field, including the quasistatic contribution of the current, which means that the time average value is not zero. We note that the signal is small before 25 ns, and then begins to increase rapidly. If we neglect the sub-SP diffraction background, the frequency of this signal is 9.1 GHz, the second harmonic of the sub-SP evanescent wave. In this signal one may discern two distinct behaviors. At early times (25–32 ns) there is the so-called linear regime, which is inherent in all high-gain bunching-

induced mechanisms of electromagnetic emission. Here we observe an oscillatory signal in an exponentially growing envelope, from which we shall estimate a gain coefficient. When the oscillation reaches a saturation value, exponential growth ceases, and a regime with an oscillatory envelope is observed. Saturation is usually attributed to the fact that the beam loses enough energy to fall out of resonance with the evanescent wave.

In order to study the time history of the radiation pattern, we have measured B_z as a function of time, from 5° to 175°, in steps of 1°. From the FFTs of these signals we compute the pairs of wavelengths and angles plotted in Fig. 5. We discuss this diagram in some detail. According to Andrews and Brau, CSP is expected whenever a SP frequency coincides with a harmonic of the evanescent wave. The first and second order SP wavelengths are shown in the figure as a function of angle. Where they intersect the horizontal lines corresponding to the second and third harmonics, one expects CSP. First, we observe CSP around the expected angle of 78° at frequency 9.1 GHz (second harmonic). Second, the expected third harmonic at 13.2 GHz is also seen, and the angular distribution peaks at both the first order angle of 40° and the second order angle of 115°. The scale on the right shows the FFT amplitudes as a function of angle at the corresponding frequencies. We find these results provide strong support for the approach of Brau and his colleagues.

The bunching can be observed as a function of both space and time. We show in Fig. 6(a) the beam current as a function of x, for times 24, 26, and 28 ns, respectively. The bunching is clearly periodic at the sub-SP value, $2\pi/k \cong 3.54$ cm. However, higher spatial harmonics are also present. In Fig. 6(b) we have plotted the current as a function of t at three values of x. The top curve corresponds to the beam current at the second period, the middle curve
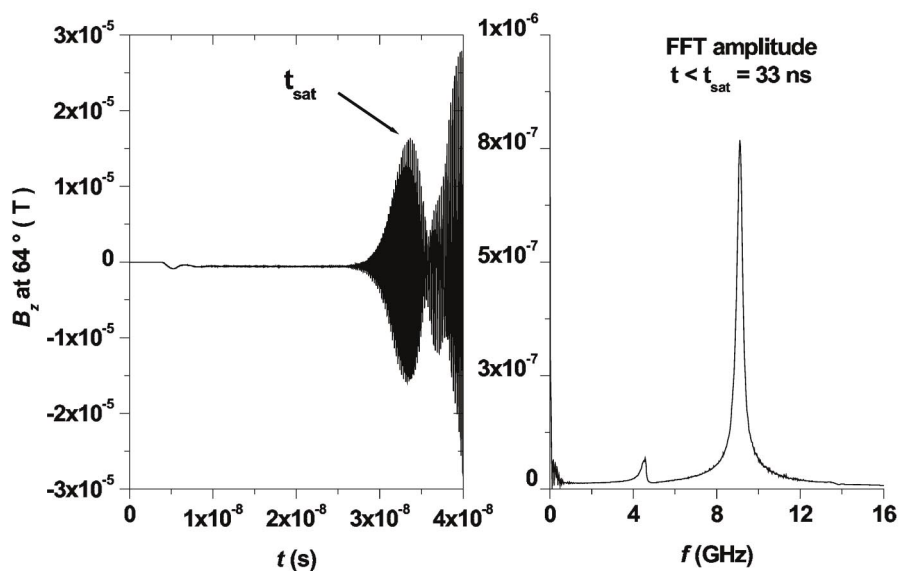

FIG. 4.   Time signal of B_z and corresponding FFT from a detector placed at 64°.
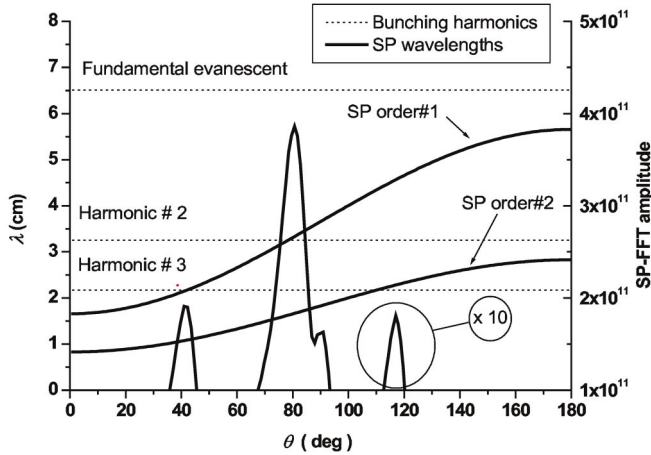
FIG. 5. Amplitude of the major FFT coefficients as a function of angle. Also shown are the first and second order SP wavelengths as a function of angle, together with the wavelengths of the fundamental (evanescent), second, and third harmonics.

is for the grating center, and the bottom curve is for two periods short of the downstream end. We note that the beam is unbunched near the entry for all times, and that the strong bunching at the downstream end occurs earlier than in the middle. In fact, if one looks at CSP radiation at early times, the center of emission appears to be close to the downstream end, where the bunching is strongest. The
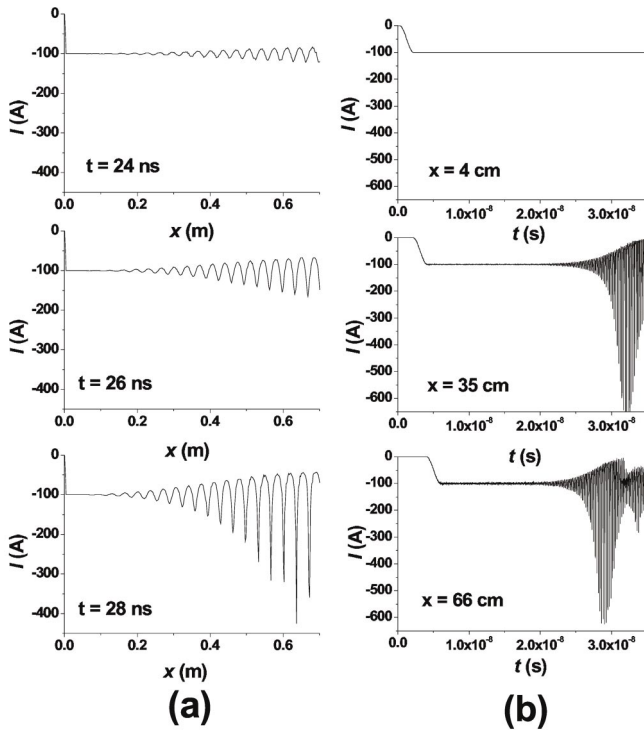
FFTs of these signals show that the beam is strongly bunched at the sub-SP frequency and at several harmonics of 4.57 GHz.

We present in Fig. 7 another way to observe the beam bunching: phase-space plots at time 32 ns. Figure 7(a) shows the density of electrons in the x-y plane when bunching has occurred and Fig. 7(b) shows the density in kinetic energy-x phase space. Appreciable energy modulation is visible. The spatial density modulation at wavelength 3.54 cm is observed again. At the downstream end, the electron energy distribution has become largely concentrated around two values, 110 and 70 keV, with few in between. This could develop into the well-known two-stream instability, and cause loss of output.

Although most aspects of our simulation tend to support the Andrews and Brau model of CSP, one major feature came as a surprise. In Fig. 8(a) we show three contour maps in the x-y plane of the magnetic field B_z in the region just above the grating. They correspond to times of 30, 32, and 34 ns, respectively. Visual inspection shows that successive maxima are separated by about 4.8 cm. This is clearly different from the periods of 3.54 cm seen in the current and phase-space profiles in x. In order to investigate this in greater detail, we plotted B_z as a function of x for fixed $t =$

FIG. 6. (a) Current as a function of x at three different times. (b) Current as a function of time at three different locations along the grating.
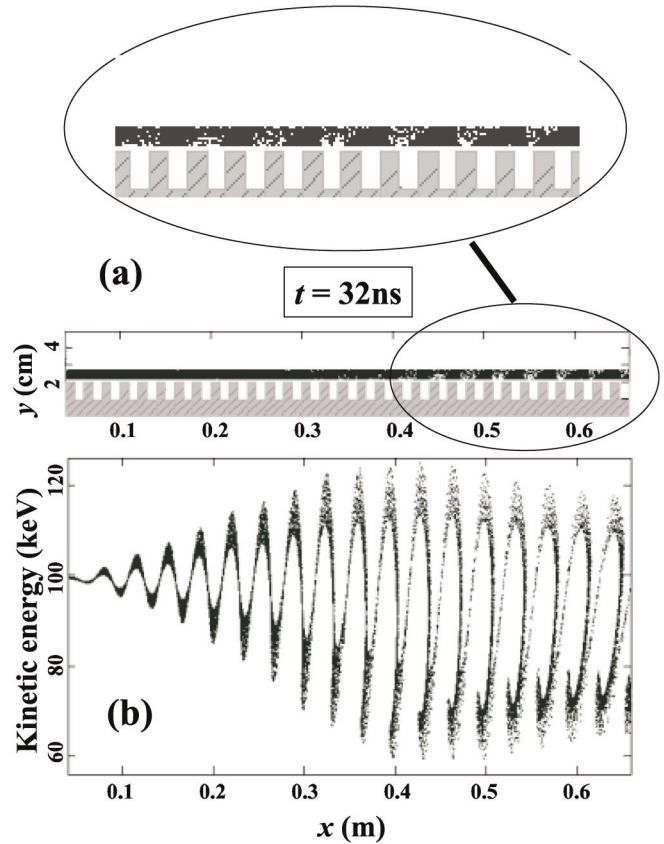

FIG. 7. Projected phase-space distributions: (a) density of electrons in the x-y plane at 32 ns. Bunching is evident. (b) kinetic energy-x density at same time.
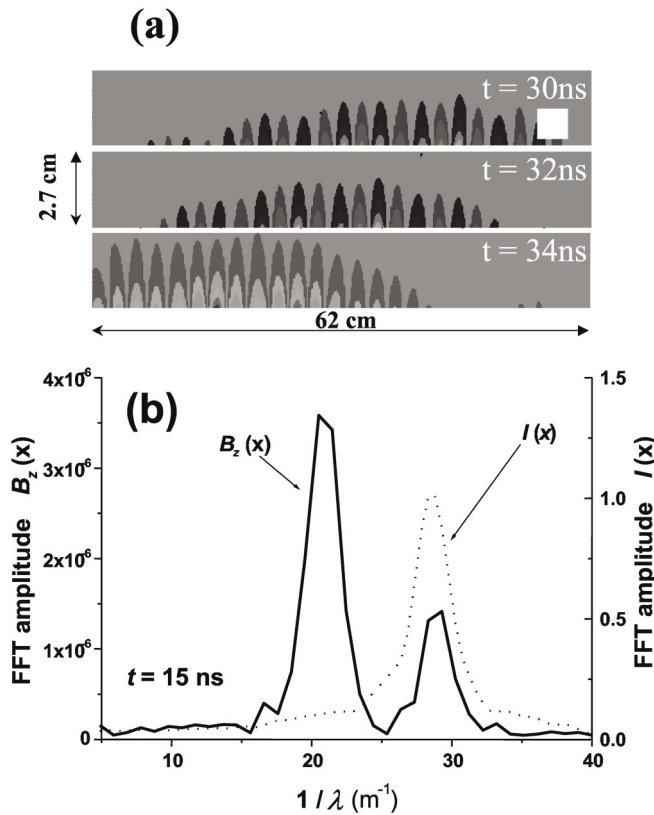
FIG. 8. (a) $B_z(x)$ near the grating at three different times, showing an approximate period of 4.8 cm, and indicating a slow movement in the negative x direction. (b) FFT of $B_z(x)$ (solid curve, with two peaks) compared to FFT of current (dashed curve, one peak).

15 ns and $y = 2.5$ cm (inside the beam). From this we obtained the spatial FFT displayed in Fig. 8(b). For comparison we show a similar FFT of the current at the same time (dotted curve, scale on right). The FFT variable is $k/2\pi$, the inverse wavelength of the oscillation. The FFT of B_z has two peaks. That at 21 m^{-1} corresponds to the 4.8 cm suggested by the contour maps, whereas the second occurs at the same place as the peak in the current FFT, approximately 3.5 cm, in good agreement with the apparent period in Fig. 6. If we refer to Fig. 2, we note that the dispersion relation has two solutions for a given value of ω, that we called k and k'. Our FFT does not distinguish the sign of the wave number, but from the contour maps one sees that the dominant mode is $-k'$. In addition, the maps clearly show a localized structure which moves in the negative x direction. One may estimate its speed to be about -0.14. This is close to the expected group velocity for the wave number $-k'$.

C. Coherent SP Gain

A main issue of the theory of coherent SP radiation is the gain. With MAGIC, we can compute the temporal gain in two different ways. We plot the quantity $\mathrm{Re}[\ln(B_z(t))]$ vs t

at a fixed position (far away from the grating), and extract the slope of the resulting linear envelope, which is the imaginary part of the frequency, Im ω. This slope is the desired temporal gain coefficient. Alternately, we can perform an FFT of $B_z(t)$, and fit at the peak in the power spectrum to the Breit-Wigner formula. The full-width at half maximum is Im ω/π. We verify that these two methods agree, within errors. Furthermore, a similar treatment can be applied to the time variation of beam current at the end of the grating.

We have varied the beam current I over a range from 25 to 1500 A. For each value, we have found the gain which is shown in Fig. 9(a). In fact, we are analyzing the B_z signal at the main peak near 78°, which is at the second harmonic of the evanescent wave. A least squares fit to the points assuming the $I^{1/3}$ form yields the result $0.2 \times 10^9 I^{1/3}$ s^{-1}. In Fig. 9(b) we show the corresponding variation of the CSP radiation frequency with the current. A linearly decreasing frequency is observed when the current is increased. This is due to space charge which reduces the value of the particle velocity, reducing the slope of the
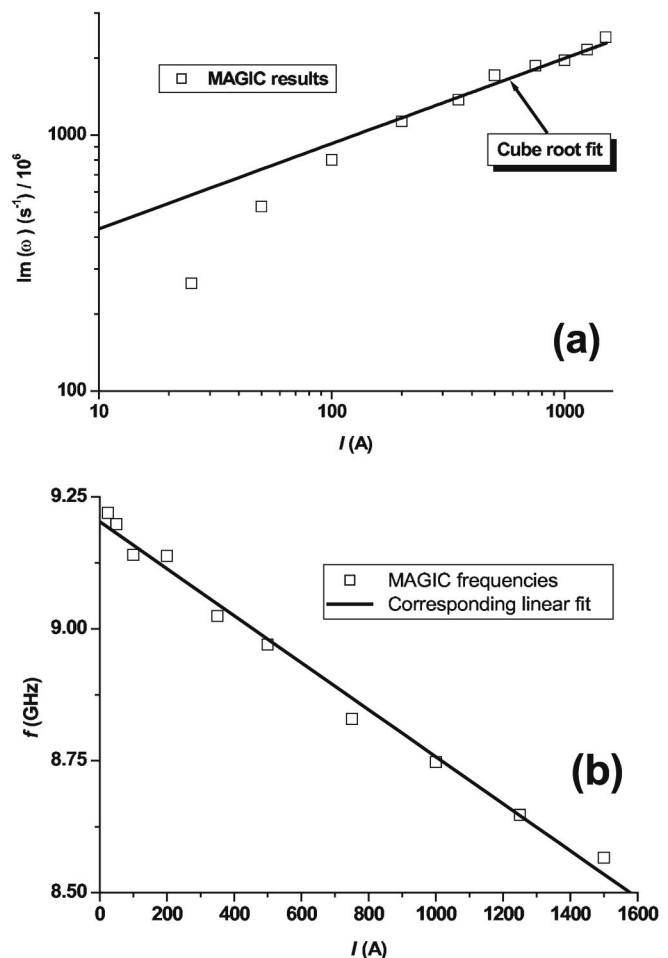

FIG. 9. (a) Temporal gain Im (2ω) as a function of current (b) CSP frequency as a function of current.

beam line in Fig. 2. The intersection is shifted to smaller ω and larger k as the current increases. It should be noted that the numerical determination of the gain is neither trivial nor error free. At low currents extremely long computation times are needed to produce an observable signal. In contrast, at high current, the signal rises so rapidly that it is hard to tell when saturation occurs, thereby making the slope estimation difficult.

The formula proposed by Andrews and Brau in Ref. [12] yields the numerical value, $|\text{Im}\,k| = 0.0275 I^{1/3}$ cm^{-1} for the spatial gain of the evanescent wave. Our MAGIC based evaluation, using the currents shown in Fig. 6 yields $|\text{Im}\,k| = 0.014 \pm 0.002\,(I)^{1/3}$ cm^{-1}. This is a factor of 2 less than the prediction, but the order of magnitude is correct. The formula given by Schäcter and Ron yields rather similar values with our conditions, although this need not be the case. We evaluate their prediction to be $|\text{Im}\,k| = 0.0313 I^{1/3}$ cm^{-1}, which is again somewhat more than what we find.

The problem of gain and attenuation has received a more extensive treatment in a recent preprint by Andrews, Boulware, Brau, and Jarvis [18]. They point out that in CSP radiation, the instability which leads to wave growth may be either convective (growth as a function of distance along the grating, Im k) or absolute (growth in time, Im ω). They show that if the intersection of the beam line and the dispersion relation occurs on the low side of the peak (see Fig. 2), the convective instability is expected, while for an intersection on the high side, the instability is absolute. They also point out that the maximum $|\text{Im}\,k|$ occurs for real values of frequency. It is clear from our results on the current (see Fig. 6) that we have both spatial and temporal growth, and we have determined numerically the corresponding Im k, and Im ω, at the fundamental frequency. We can also estimate Im ω from our observations of the field $B_z(t)$ at distance points as a function of time. The presence of waves near the grating with two distinct wave numbers and propagating in both directions makes it impossible to get reliable estimates of Im k for these waves. In their discussion of the absolute instability, the authors derive the equation

$$(\delta\omega - \beta_g \delta k)(\delta\omega - \beta_b \delta k)^2 = \Delta/(cK)^3, \qquad (2)$$

where $\delta\omega$ is the frequency shift (in units of cK), δk is the wave number shift (in units of K), β_g is the relative group velocity of the grating wave, β_b is the relative beam (or phase) velocity, and Δ is a real positive quantity proportional to the current density. For our simulation, the dimensionless quantity $\Delta/(cK)^3$ has the numerical value $4.73 \times 10^{-8} I$, where the current I is in amperes. We then impose that Im k have the value we find at 100 A, -0.06 ± 0.01/cm, and solve the equation for ω as a function of Re k, for small values of the latter. Only one root of the cubic has a positive imaginary part, and for Re $k = -0.07$ we obtain a value of Im ω close to that observed, $0.4 \times$

10^9 s^{-1}. The corresponding shift in Re ω is -1.2×10^9 s^{-1}. The unperturbed ω is 28.9×10^9 s^{-1}, so that the shift represents a few percent. The authors of Ref. [17] proceed differently, imposing boundary conditions on the solution of the cubic. Our less ambitious approach simply shows that our results for the spatial and temporal growth are not inconsistent with Eq. (2).

IV. DISCUSSION

In Sec. I, we referred to theories of SP radiation, and our intention was to compare these with the results of our simulation. The most significant conclusion we draw is that the analysis of Andrews and Brau is strongly supported by the results of our simulation. For small beam currents, where the space charge associated with the beam does not substantially reduce the initial velocity of the beam, the beam bunching occurs at the frequency ω and wave number k that are quite close to those that the Andrews-Brau analysis predicts. Coherent SP radiation is observed at those angles for which the SP frequency coincides with an integer multiple of the frequency of the evanescent wave, again a definite prediction of the model. The gain we observe is within a factor of 2 of that predicted by the Andrews-Brau model, although the prediction of Schächter and Ron is not much farther off. We are unable to rule out the possibility that the gain increases as $I^{1/2}$, mainly because of the difficulties of measuring the gain in simulations at both very low and very high currents.

Despite the overall success of the Andrews-Brau model, it does not address the question of what happens at the end of the grating (simply because an infinitely long grating was assumed). Our simulation suggests that what happens at the ends is of great importance for understanding the copious amount of sub-SP radiation that we see. Reasoning by analogy with an open ended wave guide, we expected the incident evanescent wave moving in the positive x direction to radiate some energy and to undergo some amount of reflection into a wave moving in the negative direction. However, we cannot see this reflected signal (wave number $= -k$) because of the considerably larger signal at wave number $-k'$. We assume, but cannot yet prove, that the latter arises also by reflection first at the downstream end, then bounces back and forth emitting copious sub-SP radiation at each end of the grating. Although the existence of this mode is predicted in the Andrews-Brau framework, its importance in our simulation was not foreseen. The fact that no experiments have seen such radiation remains an unsolved problem. Our best guess is that in a 3D situation the radiation at the ends might be emitted into a broad solid angle and escape detection, whereas our simulation suggests it should be seen at practically all angles. A 3D simulation should be able to address the question.

Our simulation shows that the beam loses several percent of its energy (10^7 W per vertical meter). Since we

have no dissipation, all of this energy must ultimately appear as radiation, mainly at the sub-SP frequency. At the second harmonic, using the early peak value of 0.000 015 T for the magnetic field at 78° at 85 cm from the center [Fig. 6(a)], we estimate the power radiated to be approximately 5000 W per vertical meter. This is approximately 0.0005 of the beam power. Since we have observed exponential gain, it appears plausible that a somewhat longer grating would be more efficient. However, the saturation we observe, followed by strong fluctuations in intensity, suggests that the operation of a Smith-Purcell FEL in a continuous manner may not be an easy task. In contrast pulsed operation should be relatively straightforward. We plan to study the optimization of the system, varying parameters so as to seek a quasistable mode of operation.

ACKNOWLEDGMENTS

[1] S. J. Smith and E. M. Purcell, Phys. Rev. **92**, 1069 (1953).
[2] P. M. van den Berg, J. Opt. Soc. Am. **63**, 689 (1973).
[3] J. M. Wachtel, J. Appl. Phys. **50**, 49 (1979).
[4] L. Schächter and A. Ron, Phys. Rev. A **40**, 876 (1989).
[5] J. Urata, M. Goldstein, M. F. Kimmitt, A. Naumov, C. Platt, and J. E. Walsh, Phys. Rev. Lett. **80**, 516 (1998).
[6] O. Kapp, Yin-e Sun, Kwang-Je Kim, and A. V. Crewe, Rev. Sci. Instrum. **75**, 4732 (2004).
[7] C. Brau (private communication).
[8] G. Kube *et al.*, Phys. Rev. E **65**, 056501 (2002).
[9] A. Doria *et al.*, Nucl. Instrum. Methods Phys. Res., Sect. A **483**, 263 (2002).
[10] Kwang-Je Kim and Su-Bin Song, Nucl. Instrum. Methods Phys. Res., Sect. A **475**, 158 (2001).
[11] H. L. Andrews and C. A. Brau, Phys. Rev. ST Accel. Beams **7**, 070701 (2004).
[12] H. L. Andrews, C. H. Boulware, C. A. Brau, and J. D. Jarvis, in *Proceedings of the 2004 FEL Conference, Trieste Italy*, p. 278 (http://www.JACoW.org).
[13] J. R. Pierce, *Traveling-Wave Tubes* (Van Nostrand, New York, 1950).
[14] A Bakhtyari, J. E. Walsh, and J. H. Brownell, Phys. Rev. E **65**, 066503 (2002).
[15] A. Hirata and T. Shiozawa, Electron. Commun. Jpn., Pt. 2 **80**, 30 (1997).
[16] H. P. Freund and T. M. Abu-Elfadi, IEEE Trans. Plasma Sci. **32**, 1015 (2004).
[17] D. Smithe and L. Ludeking, Comput. Phys. Commun. **106**, 95 (1997).
[18] H. L. Andrews, C. H. Boulware, C. A. Brau, and J. D. Jarvis, Phys. Rev. ST Accel. Beams **8**, 050703 (2005).